MHD Poiseuille Flow of a Jeffrey Fluid over a Deformable Porous Layer

M. Krishna Murthy
Assistant Professor, Department of Mathematics, AER Degree and P.G. College, Tirupati

Abstract
Poiseuille flow of a conducting Jeffrey fluid in a channel is investigated. The channel is bounded below by a finite deformable porous layer and bounded above by a stationary plate. The governing equations are solved in the free flow and porous flow regions. The expressions for the velocity field and solid displacement are obtained. The effects of the Jeffrey parameter, magnetic field parameter, viscosity parameter, the volume fraction component of the fluid on the flow velocity, displacement, mass flux and shear stress are discussed. It is found that the velocity increases with the increase in the non-Newtonian Jeffrey parameter whereas the velocity decreases with the increase in the magnetic field parameter.
Keywords: MHD; Poiseuille flow; Jeffrey fluid; Porous layer; permeable bed.

1. INTRODUCTION
Viscous flow through and past porous media has important applications in engineering and medicine. Most of the research works in flow through porous media available deal with undeformable porous media. The work on deformable porous media is very limited. The coupled phenomenon of fluid flow and deformation of porous materials is a problem of prime importance in geomechanics and biomechanics. One application of interaction of free flow and deformable porous media, for example, is the study of haemodynamic effect of the endothelial glycocalyx.

Nomenclature

μ_a Apparent viscosity of the fluid in the porous material.	ϕ^β Volume fraction of component β and $\beta = s, f$ for the binary mixture of solid and fluid phases with $\varphi^s + \varphi^f = 1$.
K Drag coefficient.	M_d Mass flow rate in the deformable porous layer.
μ Lame constant.	M_r Mass flow rate in the non deformable porous layer.
μ_f Coefficient of viscosity.	F Fractional increase in mass flow rate.
q Fluid velocity in the free flow region in x-direction.	v Velocity of the fluid in the deformable porous layer.
u Displacement in x-direction.	δ Viscous drag.
G_0 Typical pressure gradient.	η Viscosity parameter in porous layer.
λ_1 Jeffrey parameter.	M_T Total mass flux in the channel.
M Magnetic field parameter.	B_0 Magnetic field strength
ε Porous layer thickness.	
σ Electrical conductivity	
τ_1 Shear stress.	

The study of flow through deformable porous materials was initiated by Terzaghi [1] and later continued by Biot [2,3,4] into a successful theory of soil consolidation and acoustic propagation. Atkin and Craine [5], Bowen [6] and Bedford and Drumheller [7] made important contributions to the theory of mixtures. Mow et al. [8] developed a similar theory for the study of biological tissue mechanics. Applying the theory proposed by Biot [2] water transport in the artery wall is studied by Jayaraman [9]. The same theory was also applied by Mow et al. [10], Holmes and Mow [11] for the study of rectilinear cartilages. All these works are concerned with Newtonian fluid flow through deformable porous media. Hence an attempt is made to study the effect of deformable porous layer on the classical Poiseuille flow of a Jeffrey fluid between two parallel plates.

Vajravelu et al [21] studied the influence of heat transfer on peristaltic transport of a Jeffrey fluid in a vertical porous stratum. Hayat et al. [22] studied the boundary layer flow of a Jeffrey fluid with convective boundary conditions. The effect of magnetic field on the peristaltic pumping of a Jeffrey fluid in an inclined channel is analyzed by Krishna Kumari et al. [23]. Rudraiah et al. [24] analyzed the Hartmann flow over an underormable permeable bed.

Motivated by these studies, MHD Poiseuille flow of a Jeffrey fluid between a deformable porous layer is investigated. The fluid velocity, the displacement of the solid matrix, the mass flux and its fractional increase are obtained. The effects of various physical parameters on the flow quantities are discussed through graphs.

2. MATHEMATICAL FORMULATION

Consider a steady, fully developed Poiseuille flow through a channel with solid walls at $y=-L$ and $y=h$ and deformable porous layer of thickness L attached to the lower wall as shown in Fig.1. The flow over the deformable layer is bounded above by a stationary plate. The flow region between the plates is divided into two regions. The flow region between the lower plate $y=-L$ and the interface $y=0$ is termed as deformable porous layer whereas the flow region between the interface $y=0$ and the upper plate $y=h$ is designated as free flow region. The fluid velocity in the free flow region and the porous flow region are assumed to be $(q,0,0)$ and $(v,0,0)$ respectively. The displacement due to the deformation of the solid matrix is taken as $(u,0,0)$. A pressure gradient $\frac{\partial p}{\partial x}=G_0$ is applied, producing an axially directed flow in the channel. Further a uniform transverse magnetic field of strength B_0 is applied perpendicular to the walls of channel.

In view of the assumptions mentioned above, the equations of motion in the deformable porous layer and free flow region are [25,26].

$$\mu\frac{\partial^2 u}{\partial y^2}-\phi^s G_0+K v=0, \tag{1}$$

$$\frac{2\mu_a}{1+\lambda_1}\frac{\partial^2 v}{\partial y^2}-\phi^f G_0-K v-\sigma B_0{}^2 v=0 \tag{2}$$

$$\frac{\mu_f}{1+\lambda_1}\frac{\partial^2 q}{\partial y^2}-\sigma B_0^2 q=G_0 \tag{3}$$

The boundary conditions are

at $y=-L$: $v=0,\ u=0$

at $y=0$: $q=\phi^f v$

$$\phi^f\mu_f\frac{dq}{dy}=2\mu_a\frac{dv}{dy}$$

$$\mu_f\frac{dq}{dy}=\frac{\mu}{\phi^s}\frac{du}{dy}$$

at $y=h$: $q=0$ (3)'

3. NON-DIMENSIONALIZATION OF THE FLOW QUANTITIES

It is convenient to introduce the following non-dimensional quantities.

$$y=h\hat{y},\quad u=-\frac{h^2G_0}{\mu}u,\ \ v=-\frac{h^2G_0}{\mu_f}\hat{v},\ q=-\frac{h^2G_0}{\mu_f}q,\ \varepsilon=\frac{L}{h},\ \hat{\tau}=-\frac{\tau}{hG_0}$$

In view of the above dimensionless quantities, the equations (1) – (3)' takes the following form after the hats $(\wedge)$ are neglected.

$$\frac{d^2u}{dy^2}=-\phi^s-\delta v \tag{4}$$

$$\frac{d^2v}{dy^2}=(1+\lambda_1)\eta\left[(\delta+M^2)v-\phi^f\right] \tag{5}$$

$$\frac{d^2q}{dy^2}-M^2(1+\lambda_1)q=-(1+\lambda_1) \tag{6}$$

where $M^2 = \dfrac{\sigma B_0^2 h^2}{\mu_f}, \delta = \dfrac{Kh^2}{\mu_f}, \quad \hat{G} = \dfrac{G}{G_0}, \quad \eta = \dfrac{\mu_f}{2\mu_a}, \quad G_0 = \dfrac{dp}{dx}.$

The parameter δ is a measure of the viscous drag of the outside fluid relative to drag in the porous medium. The parameter η is the ratio of the bulk fluid viscosity to the apparent fluid viscosity in the porous layer.

The boundary conditions are

at $y = -\varepsilon$: $v = 0, u = 0$ (7a)

at $y = 0$: $q = \phi^f v$

$$\frac{dq}{dy} = \frac{1}{\eta\phi^f}\frac{dv}{dy}$$

$$\frac{dq}{dy} = \frac{1}{\phi^s}\frac{du}{dy}. \tag{7b}$$

at $y = 1$: $q = 0$ (7c)

4. SOLUTION OF THE PROBLEM

Equations (4) - (6) are coupled differential equations that can be solved by using the boundary conditions (7). The solid displacement and fluid velocities in the free flow region and deformable porous layer are obtained as:

$$u(y) = -(1-\phi^f)\frac{y^2}{2} - \frac{\delta c_3 e^{by}}{b^2} - \frac{\delta c_4 e^{-by}}{b^2} - \frac{\phi^f \delta}{\delta + M^2}\frac{y^2}{2} + c_5 y + c_6 \tag{8}$$

$$q(y) = c_1 e^{ay} + c_2 e^{-ay} + \frac{1}{M^2} \tag{9}$$

$$v(y) = c_3 e^{by} + c_4 e^{-by} + \frac{\varphi^f}{\delta + M^2} \tag{10}$$

where $a = M\sqrt{(1+\lambda_1)}$ and $b = \sqrt{((1+\lambda_1)\delta + a)\eta}$ the constants c_1, c_2, c_3, c_4, c_5 and c_6 found from the boundary conditions, are

$$A_1 = \frac{(1-e^a)}{M^2} - \frac{(\phi^f)^2}{\delta + M^2},\ A_2 = \frac{b(1-e^{2a})}{\eta\phi^f} - a(1+e^{2a})\phi^f,\ A_3 = \frac{b(1-e^{2a})}{\eta\phi^f} + a(1+e^{2a})\phi^f,$$

$$A_4 = aA_1(1+e^{2a}) - \frac{ae^a(1-e^{2a})}{M^2},\ c_1 = \frac{(c_3+c_4)\phi^f - A_1}{1-e^{2a}},\ c_2 = -\left(c_1 e^{2a} + \frac{e^a}{M^2}\right),$$

$$c_3 = -\frac{\left(A_4 e^{b\varepsilon} + \dfrac{A_3\phi^f}{\delta + M^2}\right)}{A_2 e^{b\varepsilon} + A_3 e^{-b\varepsilon}}, \qquad c_4 = -\left(c_3 e^{-b\varepsilon} + \frac{\phi^f}{\delta + M^2}\right)e^{-b\varepsilon},$$

$$c_5 = \left(a(1-\phi^f)(c_1 - c_2) + \frac{\delta(c_3 - c_4)}{\eta}\right),$$

$$c_6 = \frac{\delta}{b^2}\left(c_3 e^{-b\varepsilon} + c_4 e^{b\varepsilon}\right) + \frac{\varepsilon^2}{2}\left((1-\phi^f) + \frac{\phi^f\delta}{\delta + M^2}\right) + c_5\varepsilon$$

Mass flow rate

(i) Mass flow rate with deformable porous layer

The dimensionless mass flow rate M_d per unit width of the channel in the free flow region $(0 \le y \le 1)$ is given by

$$M_d = \int_0^1 q dy = \frac{\left(c_1 e^{a} - c_2 e^{-a} - \left(c_1 - c_2\right)\right)}{a} + \frac{1}{M^2} \tag{11}$$

(ii) Mass flow rate in absence of deformable porous layer

The fluid velocity q_r for the MHD Poiseuille flow of a Jeffrey fluid between parallel plates $y=0$ and $y=1$ is obtained on solving the equation (6) subject to the boundary conditions

at $y=0$: $q_r = 0$

at $y=1$: $q_r = 0$

It can be seen that $q_r = A\,\mathrm{e}^{a\,y} + B\,\mathrm{e}^{-a\,y} + \dfrac{1}{M^2}$

where $A = \dfrac{1-e^{-a}}{M^2\left(e^{-a} - e^{a}\right)}$, $B = -\dfrac{1}{M^2} - A$

The dimensionless mass flow rate M_r per unit width of the channel in the free flow region $\left(0 \le y \le 1\right)$ is given by

$$M_r = \int_0^1 q_r\, dy = \frac{\left(Ae^{a} - Be^{-a} - \left(c_1 - c_2\right)\right)}{a} + \frac{1}{M^2} \tag{12}$$

Let F denote the fractional increase in mass flow rate due to deformable porous layer and it is defined by

$$F = \frac{M_d - M_r}{M_r} \tag{13}$$

Mass Flux

Let M_T denote the dimensionless mass flow rate per unit width of the channel is

$$M_T = M_1 + M_2 \tag{14}$$

where $M_1 = \displaystyle\int_{-\varepsilon}^{0} v\, dy = \frac{c_3 - c_4}{b} - \left(\frac{c_3 e^{-b\varepsilon} - c_4 e^{b\varepsilon}}{b} - \frac{\phi^f \varepsilon}{\delta + M^2}\right)$ and

$$M_2 = \int_0^1 q\, dy = \frac{c_1 e^{a} - c_2 e^{-a} - \left(c_1 - c_2\right)}{a} + \frac{1}{M^2}.$$

Shear stress

The shear stress in the free flow region in non dimensional form is given by

$$\tau = \frac{1}{1+\lambda_1}\left(\frac{dq}{dy}\right)$$

the shear stress at the wall interface at the boundary $y=0$ is

$$\tau_1 = \left(\tau\right)_{y=0} = \frac{a}{1+\lambda_1}\left(c_1 - c_2\right) \tag{15}$$

5. RESULTS AND DISCUSSIONS

The solutions for the fluid velocities q , v in the free flow region and deformable porous layer and solid displacement of solid matrix u are evaluated numerically for different values of physical parameters such as the volume fraction of component ϕ^f , the viscous drag parameter δ , the viscosity parameter η and the thickness of lower wall ε, magnetic field parameter M, Jeffrey parameter λ_1.

The variation of fluid velocities q, v and solid displacement u in the channel is calculated for different values of Jeffrey parameter λ_1 and is shown in figures 2, 3 and 4 for fixed δ =2.0, η=0.5, $M=1$, ϕ^f =0.5and ε=0.2.We observe that the velocities q, v and solid displacement increases with the increase Jeffrey parameter λ_1.

The variation of fluid velocities q, v and solid displacement u in the channel is calculated for different values of magnetic field parameter M and is shown in figures 5, 6 and 7 for fixed δ =2.0, η=0.5, ϕ^f =0.5, $\lambda_1 = 0.1$ and ε=0.2.We observe that the velocities q, v and solid displacement decreases with the increase magnetic field parameter M.

The variation of fluid velocities in the channel q, v and solid displacement u in the channel is calculated for different values of volume fraction of component ϕ^f and is shown in figures 8, 9 and 10 for fixed δ =2.0, η =0.5, $M=1$, $\lambda_1 = 0.1$ and ε=0.2.We observe that the velocities q, v increase with the increasing ϕ^f whereas the solid displacement u decreases with the increase in ϕ^f.

The variation of fluid velocities in the channel q, v is calculated for different values of viscosity parameter η and is shown in figures 11, 12 and 13 for fixed δ =2.0, ϕ^f =0.5, $M=1$, $\lambda_1 = 0.1$ and ε=0.2. We observe that the velocities q and v increases with the increasing viscosity parameter η whereas the solid displacement u decreases with the increase in η.

The variation of mass flow rate for M_d with ϕ^f is calculated from equation (11) for different values of Jeffrey Parameter λ_1 for fixed δ =2.0, η=0.5, $M=1$ and ε=0.2 also magnetic field parameter M for fixed δ =2.0, η=0.5, $\lambda_1 = 0.1$, ε=0.2 are shown in figures 14 and 15 We observe that the mass flow rate increases with increase in the Jeffrey parameter. Further the effect of magnetic field is to reduce the mass flow rate and the rate of reduction depends on the strength of the magnetic field, which is similar to the observation made by Rudraiah et al.[24] for the Hartmann flow over a non-deformable permeable bed.

The variation of fractional increase F with ϕ^f is calculated from equation (13) and is shown in figure 16 for fixed δ =2.0, η=0.5, ε=0.2 and $\lambda_1 = 0.1$.We observe that the fractional increase decreases with increasing magnetic field parameter M.

The variation of dimensionless mass flow rate per unit width of the channel M_T with ϕ^f is calculated from equation (14) and is shown in figure 17 for fixed δ =2.0, η=0.5, ε=0.2 and $M=1$.We observe that the mass flow rate increases with increasing Jeffrey parameter λ_1.

The variation of dimensionless mass flow rate per unit width of the channel M_T with ϕ^f is calculated from equation (14) and is shown in figure 18 for fixed δ =2.0, η=0.5, ε=0.2 and $\lambda_1 = 0.1$.We observe that the mass flow rate decreases with increasing magnetic field parameter M.

The variation of shear stress τ_1 with ϕ^f is calculated from equation (15) and is shown in figure 19 for fixed $\delta = 2$, $\varepsilon = 0.2$, $M=1$ and $\eta = 0.5$.We observe that the shear stress at the wall interface decreases with increasing Jeffrey parameter λ_1.

The variation of shear stress τ_1 with ϕ^f is calculated from equation (15) and is shown in figure 20 for fixed $\delta = 2$, $\varepsilon = 0.2$, $\lambda_1 = 0.1$ and $\eta = 0.5$.We observe that the shear stress at the wall interface decreases with increasing magnetic field parameter M.

6. CONCLUSIONS:

The present study deals with MHD Poiseuille flow of a Jeffrey fluid over a deformable porous layer. The results are analyzed for different values of the pertinent parameters, namely, Jeffrey parameter, volume fraction component The findings of the problem find applications in understanding the blood (modelled as Jeffrey fluid) flow behavior near the tissue layer (modelled as a deformable porous layer). Some of the interesting findings are as follows:

1. The effect of increase in the volume fraction component ϕ^f is to enhance the fluid velocity between the parallel plates.
2. The effect of magnetic field is to reduce the fluid velocity in the free flow region whereas in the deformable porous layer, both the fluid velocity and solid displacement decreases with increasing magnetic field.
3. The flux in the free flow region increases with an increase in the Jeffrey parameter. Also opposite behavior is noticed in case of magnetic field.
4. The total mass flow rate per unit width of the channel increases with an increase in the Jeffrey parameter. Also opposite behavior is noticed in case of magnetic field.
5. The effect of increase in the magnetic field parameter and Jeffrey parameter is to reduce the shear stress at the boundary wall $y = 0$.

References

[1] Terzaghi K. Erdbaumechanik auf Bodenphysikalischen Grundlagen. Deuticke 1925.
[2] Biot MA. General theory of three-dimensional consolidation. J. Appl. Phys. 1941; 12: 155-164.
[3] Biot MA. Theory of elasticity and consolidation for porous anisotropic solid. J. Appl. Phys.1955; 26: 182-185.
[4] Biot MA. Mechanics of deformation and acoustic propagation in porous media. J. Appl. Phys.1956; 27: 240-253.
[5] Atkin RJ, Craine RE. Continuum theories of mixtures: Basic theory and historical development. Quart. J. Appl. Math. 1976; 29: 209-244.
[6] Bowen RM. Incompressible porous media models by the theory of mixtures. Int. J. Engng. Sci. 1980 ;18:1129-1148.
[7] Bedford A, Drumheller D S. Recent advances, theory of immiscible and structured mixtures. Int. J. Engng. Sci. 1983;21: 863-960.
[8] Mow VC, Holmes MH, Lai M. fluid transport and mechanical properties of articular cartilage: a review. J. Biomechanics 1984; 17: 377-394.
[9] Jayaraman G. Water transport in the arterial wall- A theoretical study. J. Biomechanics 1983; 16: 833- 840.
[10] Mow VC, Kwan MK, Lai M, Holmes MH. A finite deformation theory for non linearly permeable soft hydrated biological tissues. Frontiers in Biomechanics, Schmid Schoenbein, S. L.Y. Woo and B. w. zweifach (eds), Springer-Verlag 1985; 153-179.
[11] Holmes MH, Mow VC. The nonlinear characteristics of soft gels and hydrated connective tissues in ultrafiltration. J. Biomechanics 1990;23: 1145-1156.
[12] Sreenadh S,Krishnamurthy M,Sudhakara E,Gopi Krishna.G. Couete flow over a deformable permeable bed, (IJIRSE) International Journal of Innovative Research in Science& Enginering 2014; ISSN(Online) 2347-3207.
[13] Seddeek MA. Heat and mass transfer on a stretching sheet with a magnetic field in a viscoelastic fluid flow through a porous medium with heat source or sink. Comput Mater Sci 2007;38:781–787.
[14] Kothandapani M, Srinivas S. On the influence of wall properties in the MHD peristaltic transport with heat transfer and porous medium, Phys A. 2008; 372:4586-4591.
[15] Hayat T, Ali N. Peristaltic motion of a Jeffrey fluid under the effect of a magnetic field in a tube. Commun Non-linear Sci Numer Simul 2008;13: 1343–1352.
[16] Hayat T,Abbas Z, Pop I, Asghar S. The effects of radiation and magnetic field on the Mixed convection stagnation-point flow over a vertical stretching sheet in a porous medium. Int J Heat Mass Transfer 2010; 53:466–474.
[17] Anwar Beg O, Bakier AY, Prasad VR, Ghosh SK. Nonsimilar, laminar, steady, electricallyconducting forced convection liquid metal boundary layer flow with induced magnetic field effects. Int J Therm Sci 2009; 48(8):1596–1606.
[18] Nadeem S, Zaheer S, Fang T. Effects of thermal radiation on the boundary layer flow of a Jeffrey fluid over an exponentially stretching surface, Numerical Algorithms 2011;57: 187–205.
[19] Ghosh SK, Anwar Be´g O, Zueco J. Hydromagnetic free convection Rayleigh flow with induced magnetic field effects. Meccanica 2010; 45:175–185.
[20] Makinde OD, Aziz A. MHD mixed convection from a vertical plate embedded in a porous medium with a convective boundary condition. Int J Therm Sci 2010; 49:1813–1820.
[21] Vajravelu K, Sreenadh S, Lakshminarayana P. The influence of heat transfer on peristaltic transport of a Jeffrey fluid in a vertical porous stratum. Commun Nonlinear Sci Numer Simulat 2011; 16: 3107–3125.

[22] Hayat T, Asad S, Qasim M, Hendi AA. Boundary layer flow of a Jeffrey fluid with convective boundary conditions. Int J Numer Methods Fluids 2012; 69:1350–62.
[23] Krishna Kumari SVHN, Ramana Murthy MV, Ravi Kumar YVK, Sreenadh S. Peristaltic pumping of a Jeffrey fluid under the effect of a magnetic field in an inclined channel, Appl.Math. Sciences 2011; 5:447 – 458.
[24] Rudraiah N, Ramaiah BK, Rajasekhar BM. Hartmann flow over a permeable bed. International Journal Engineering Science 1975; 13: 1-24.
[25] Barry SI, Parker KH, Aldis GK. Fluid flow over a thin deformable porous layer. Journal of Applied Mathematics and Physics (ZAMP) 1991; 42: 633-648.
[26] Ranganatha TR, Siddagamma NG. Flow of Newtonian fluid a channel with deformable porous walls. Proc. Of National Conference on Advances in fluid mechanics 2004;49-57.

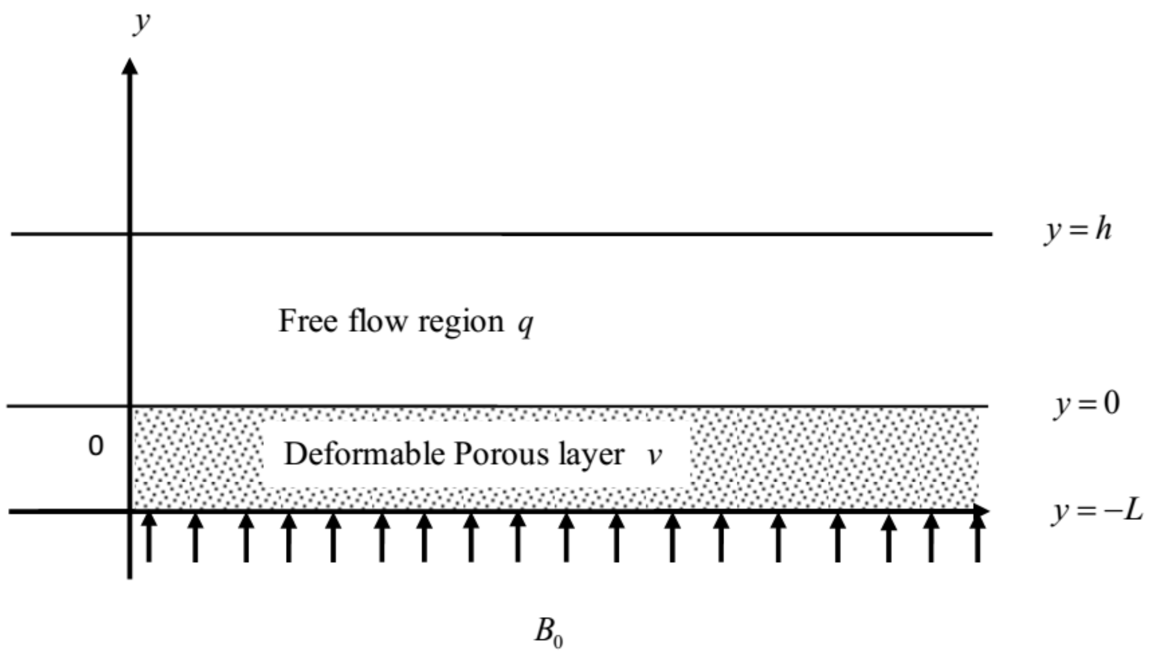

Figure 1 Physical model

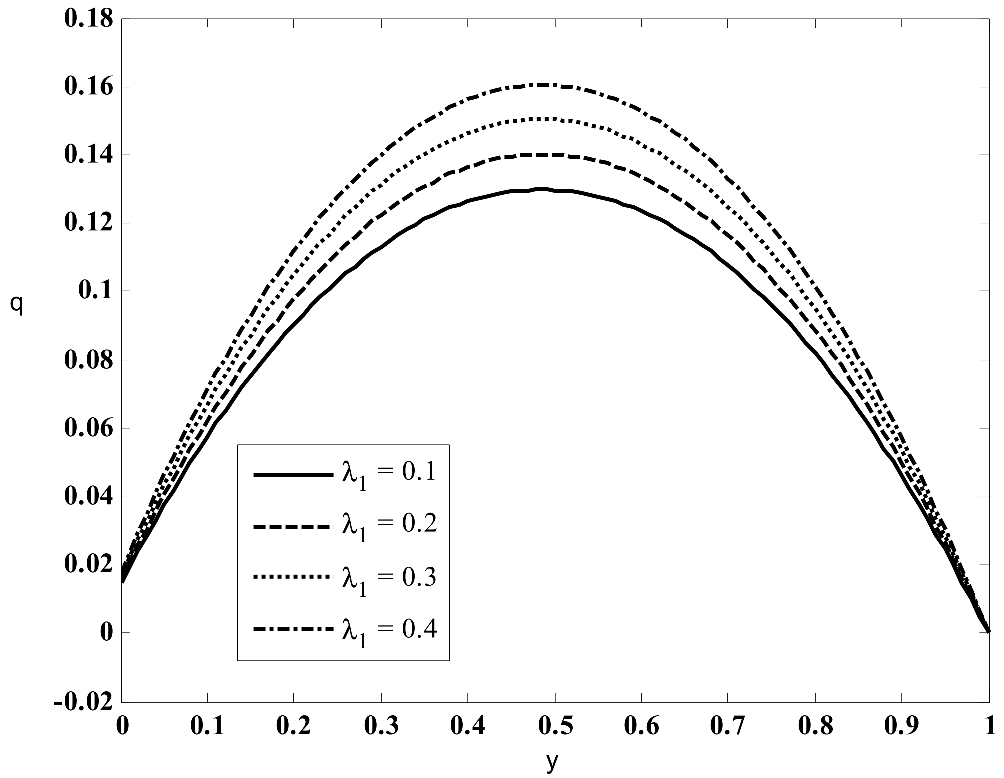

Figure 2 Velocity profiles of free flow region q for different values of λ_1.

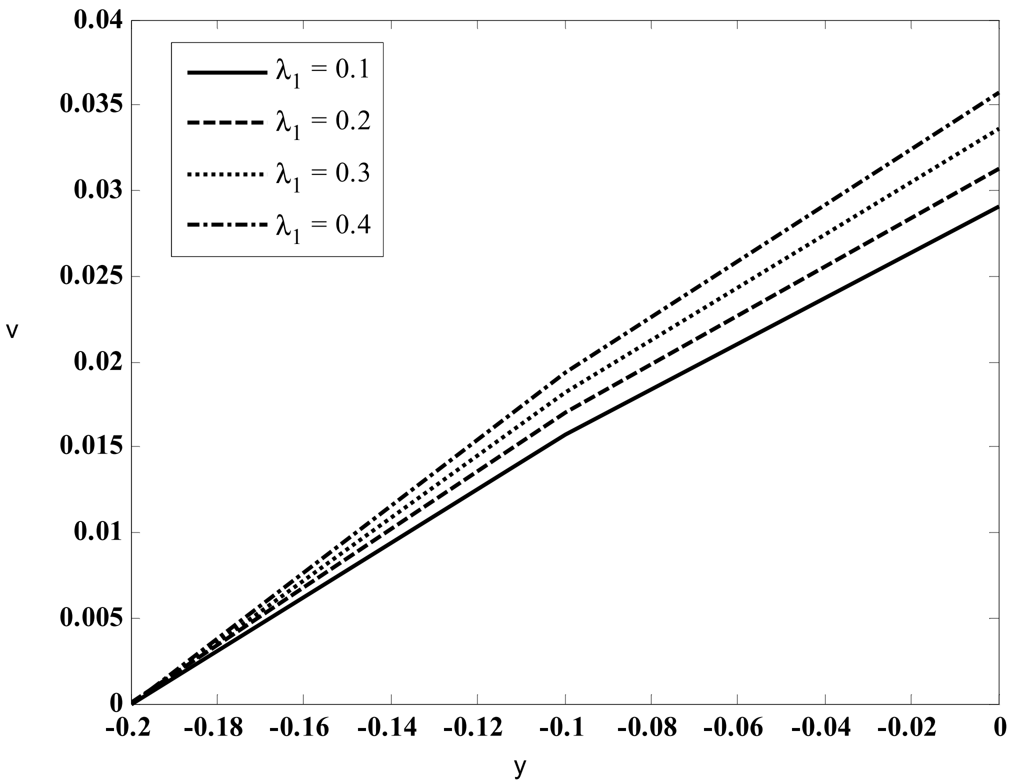

Figure 3 Velocity profiles of porous flow region v for different values of λ_1.

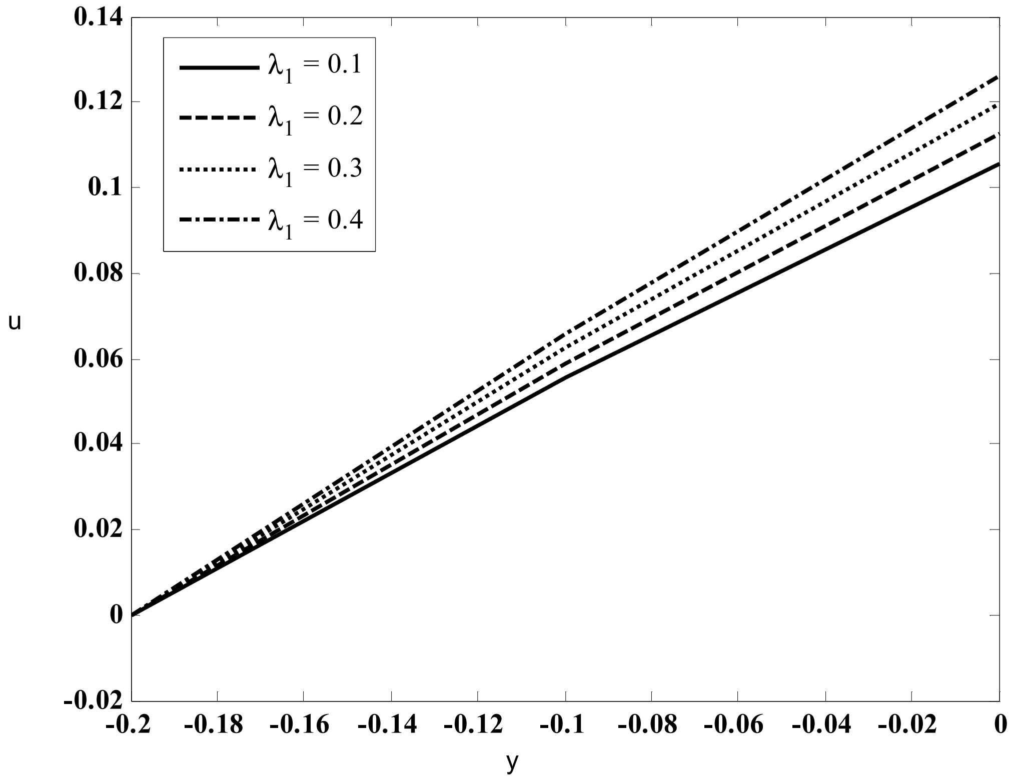

Figure 4 Velocity profiles of porous flow region u for different values of λ_1.

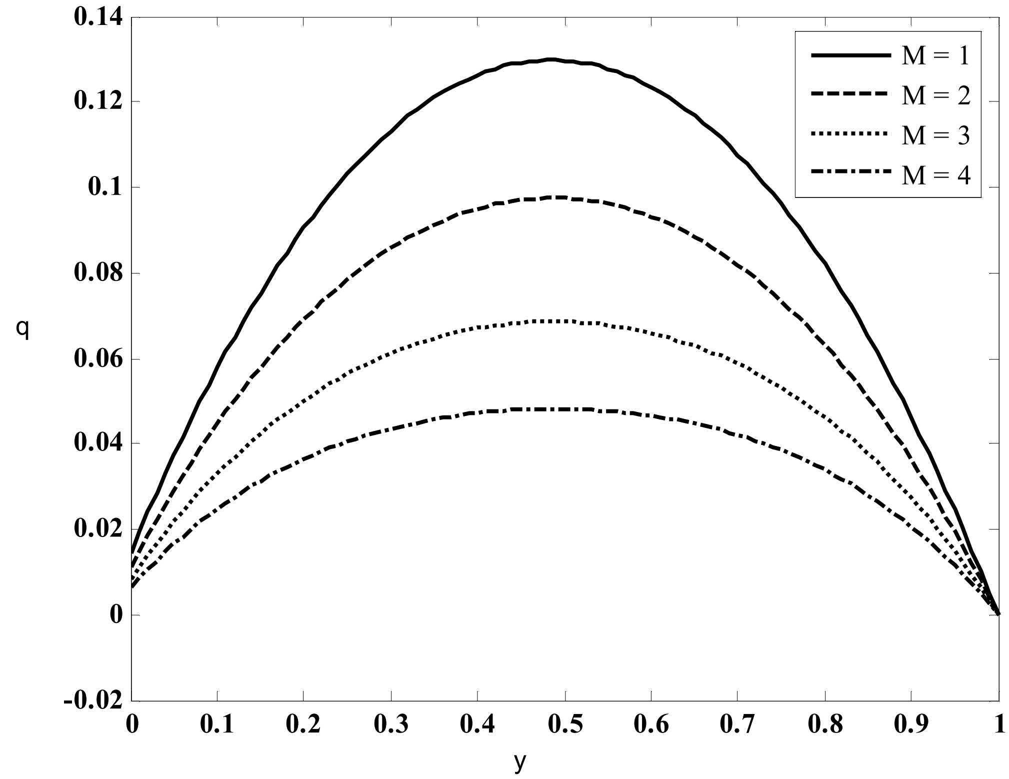

Figure 5 Velocity profiles of free flow region q for different values of M .

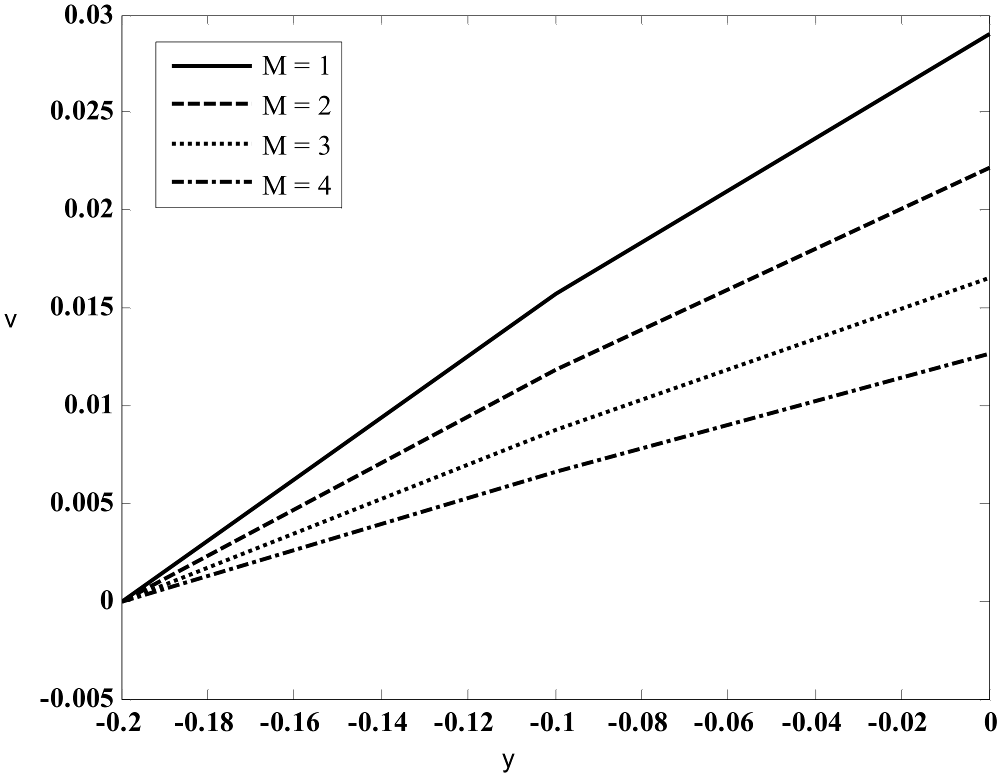

Figure 6 Velocity profiles of porous flow region v for different values of M .

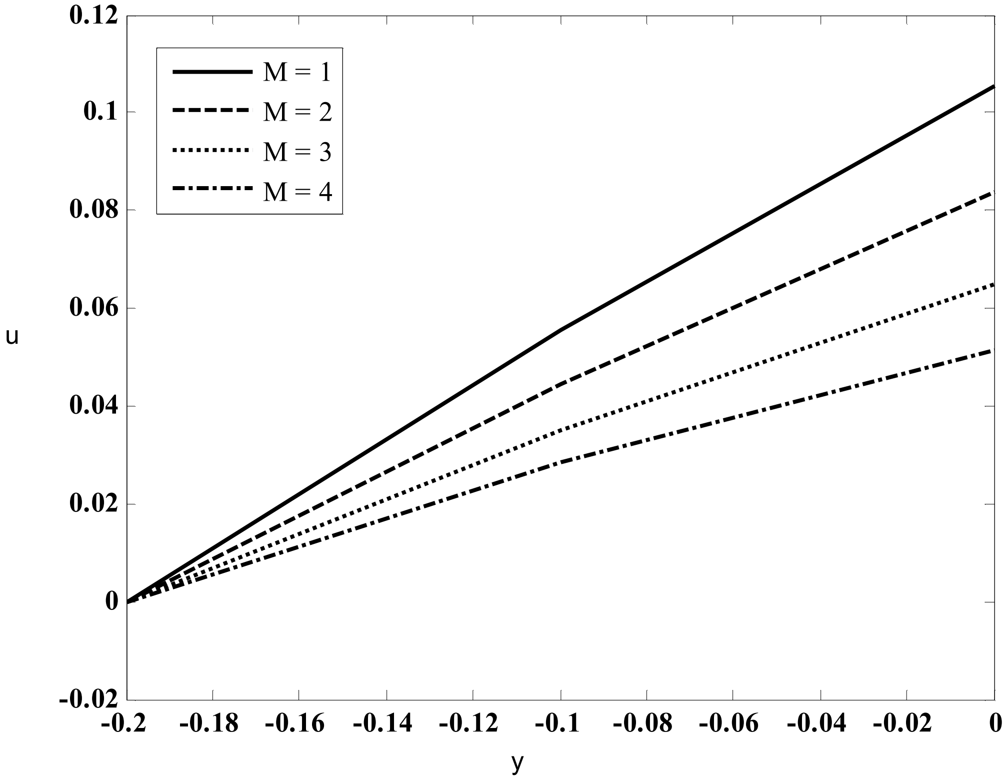

Figure 7 Velocity profiles of porous flow region u for different values of M .

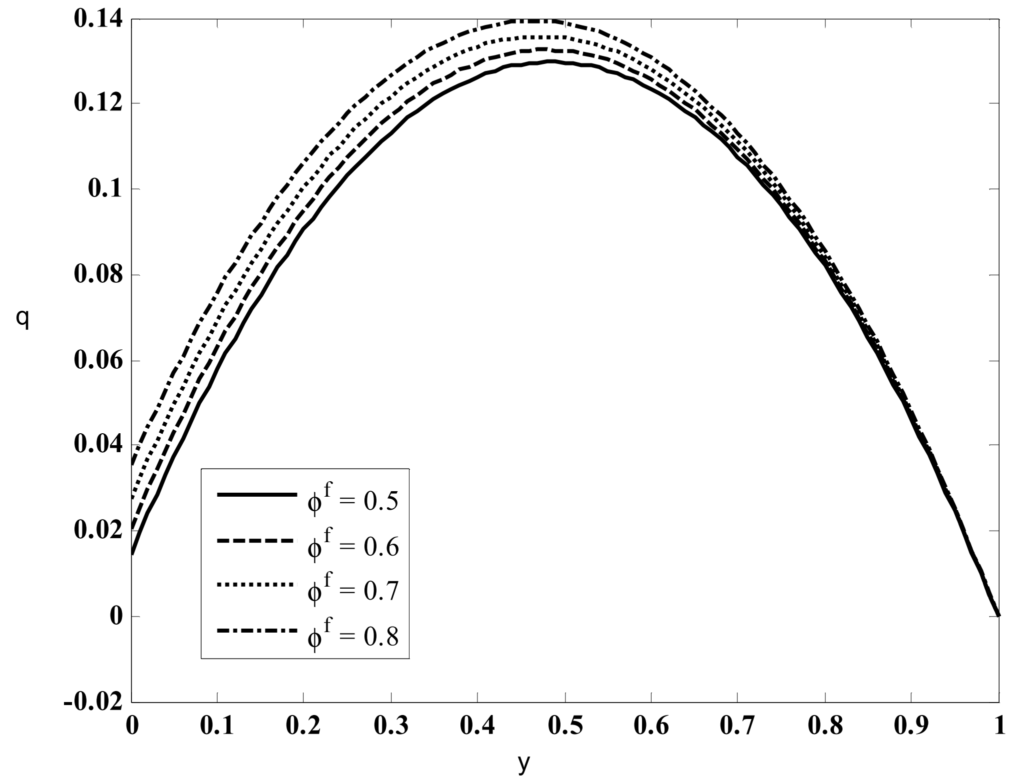

Figure 8 Velocity profiles of free flow region q for different values of φ^f .

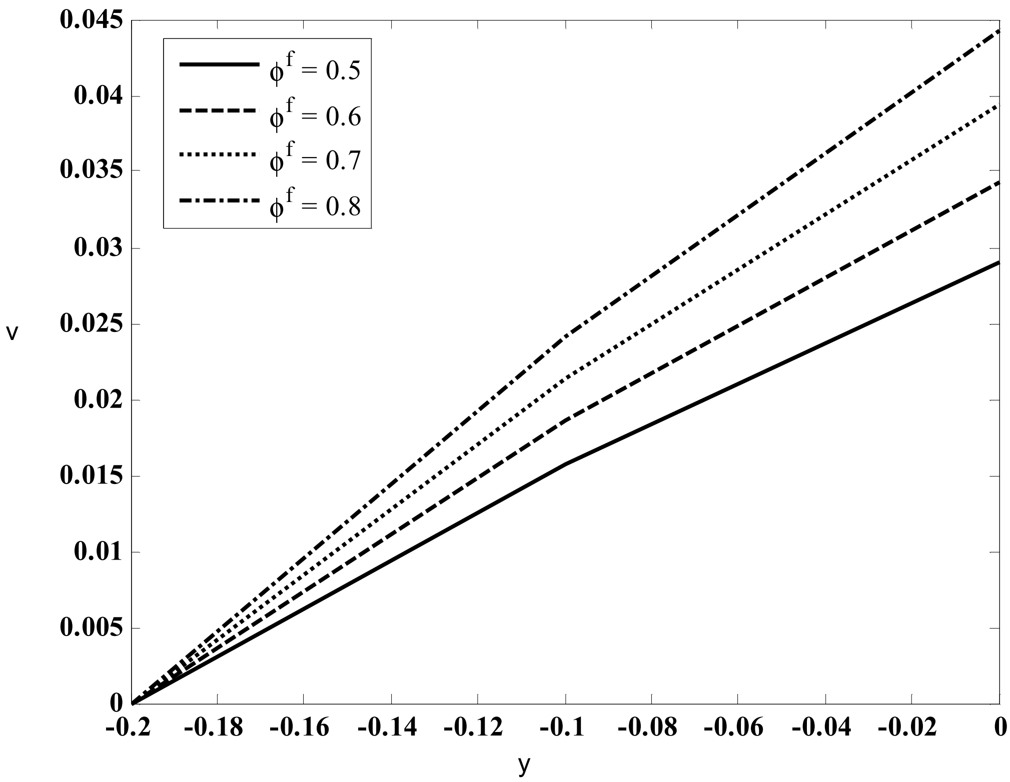

Figure 9 Velocity profiles of porous flow region v for different values of φ^f .

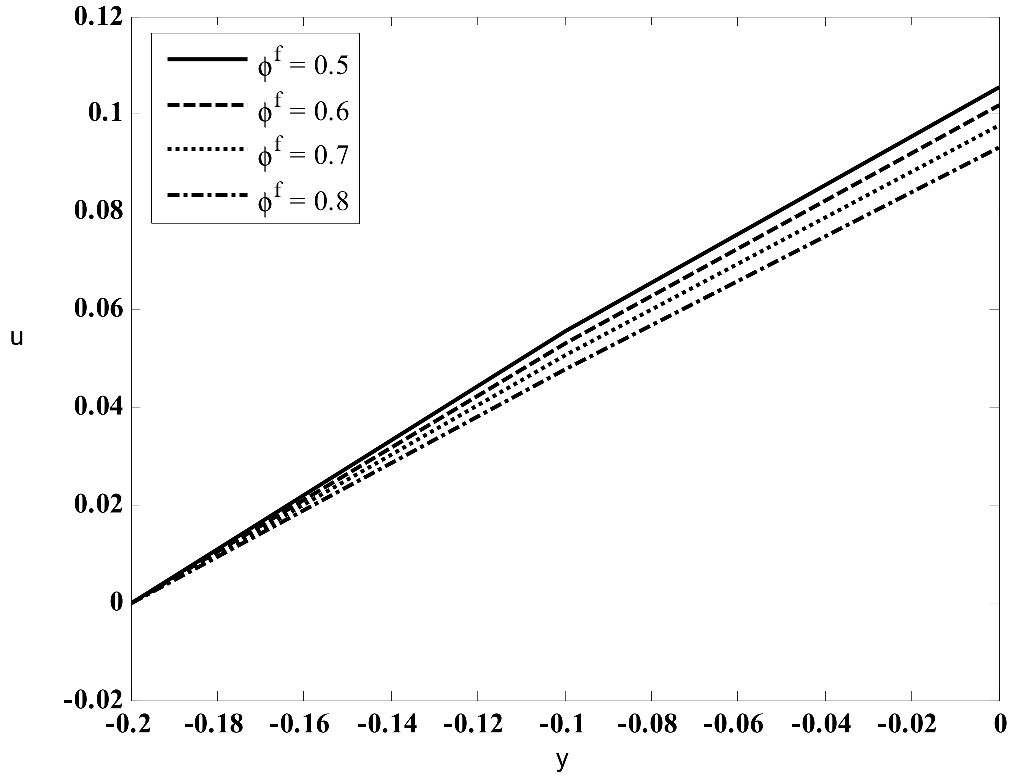

Figure 10 Velocity profiles of porous flow region u for different values of φ^f .

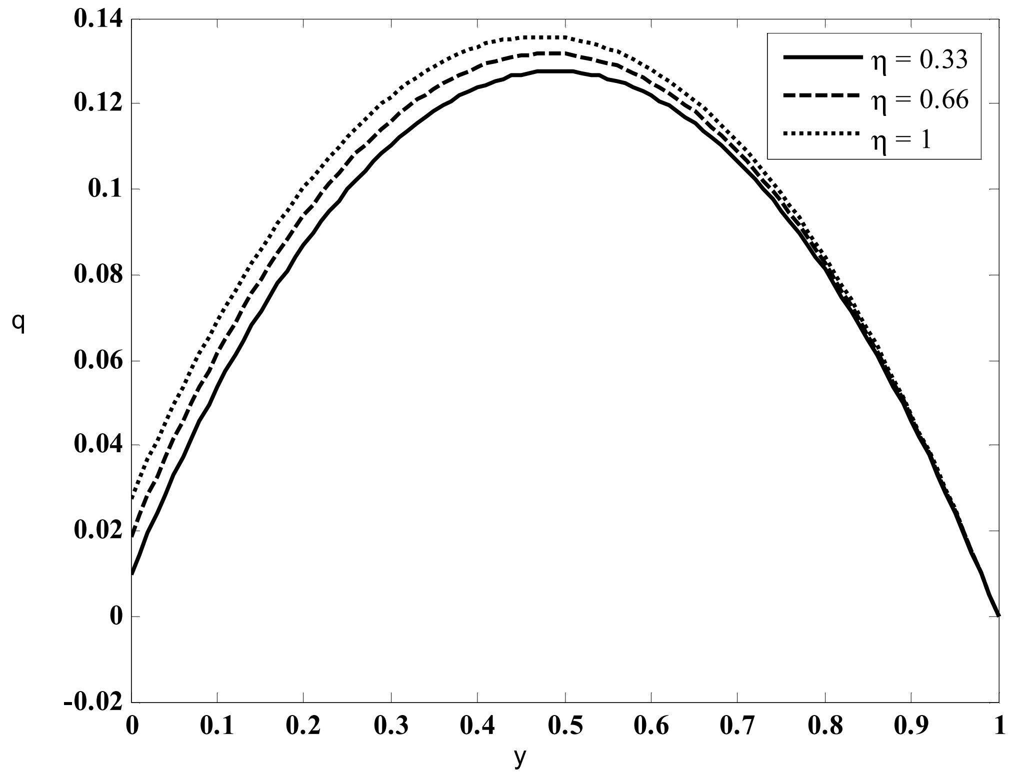

Figure 11Velocity profiles of free flow region q for different values of η .

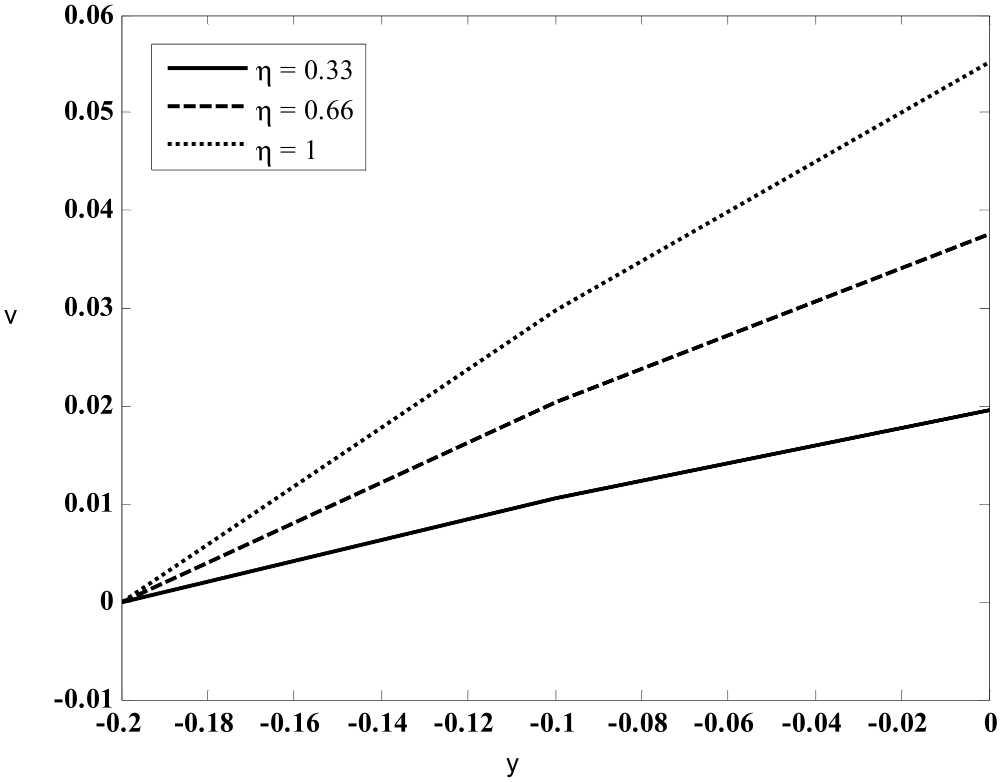

Figure 12 Velocity profiles of porous flow region v for different values of η.

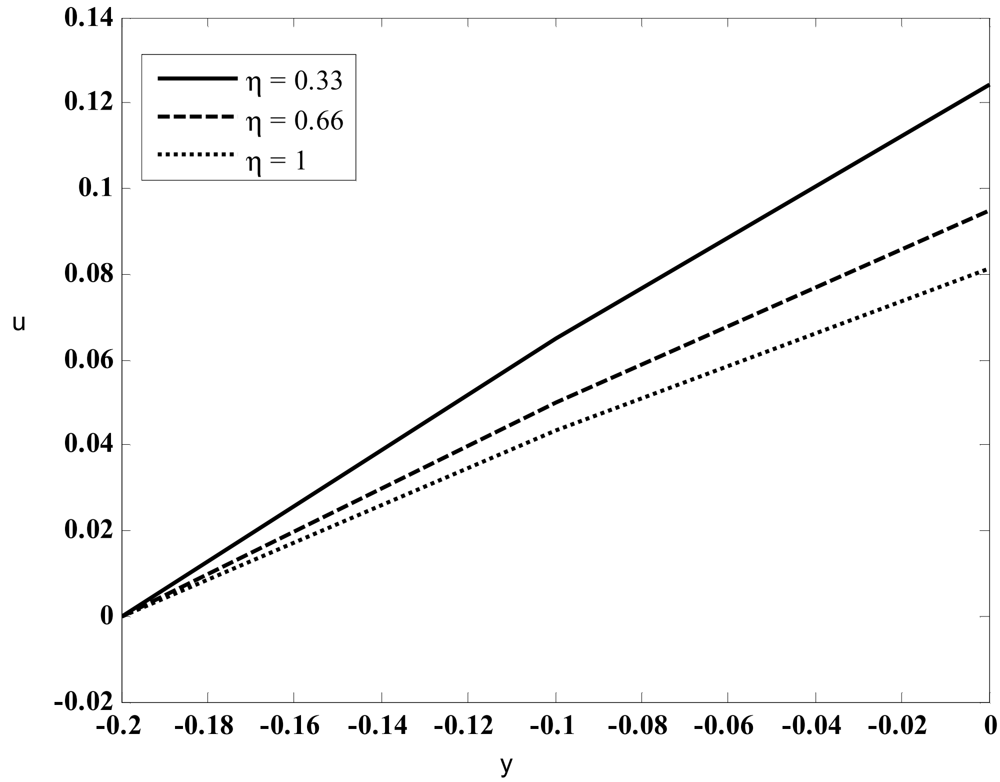

Figure 13 Velocity profiles of porous flow region u for different values of η.

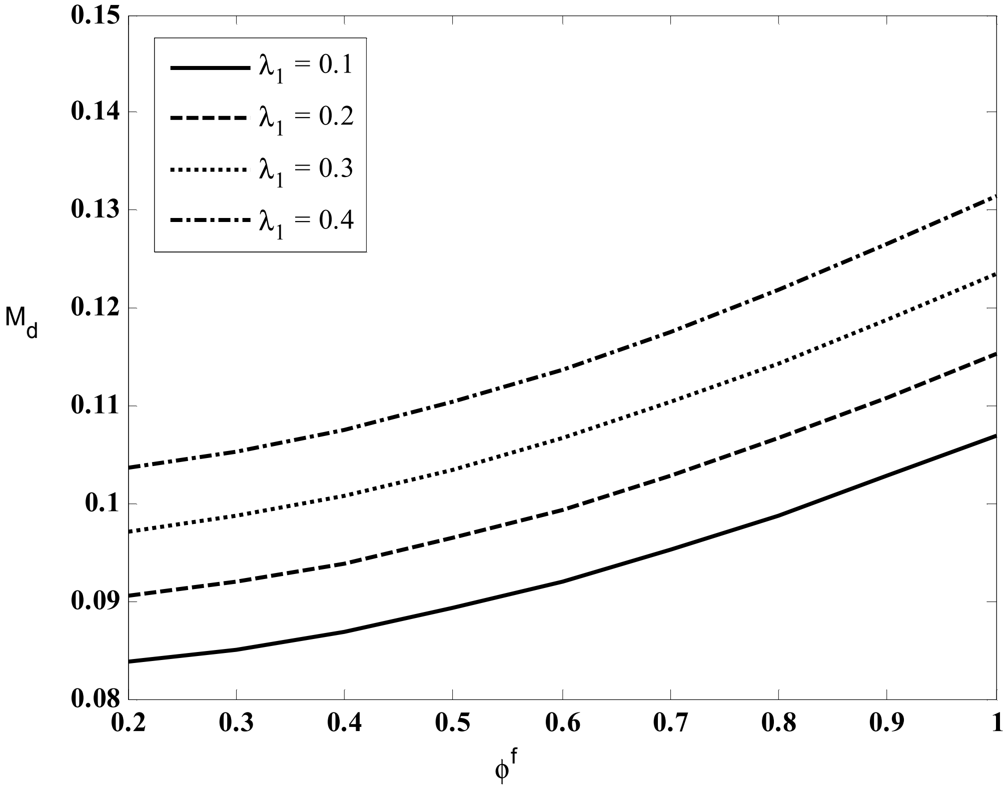

Figure 14 Variation of M_d with φ^f for different values of λ_1.

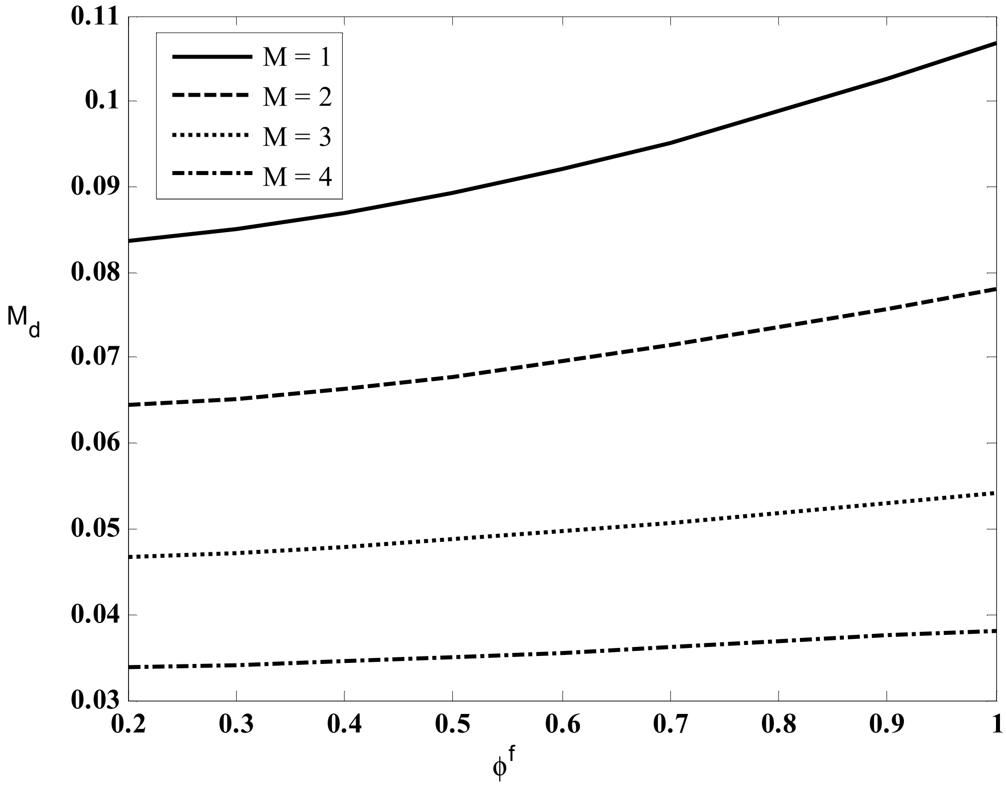

Figure 15 Variation of M_d with φ^f for different values of M .

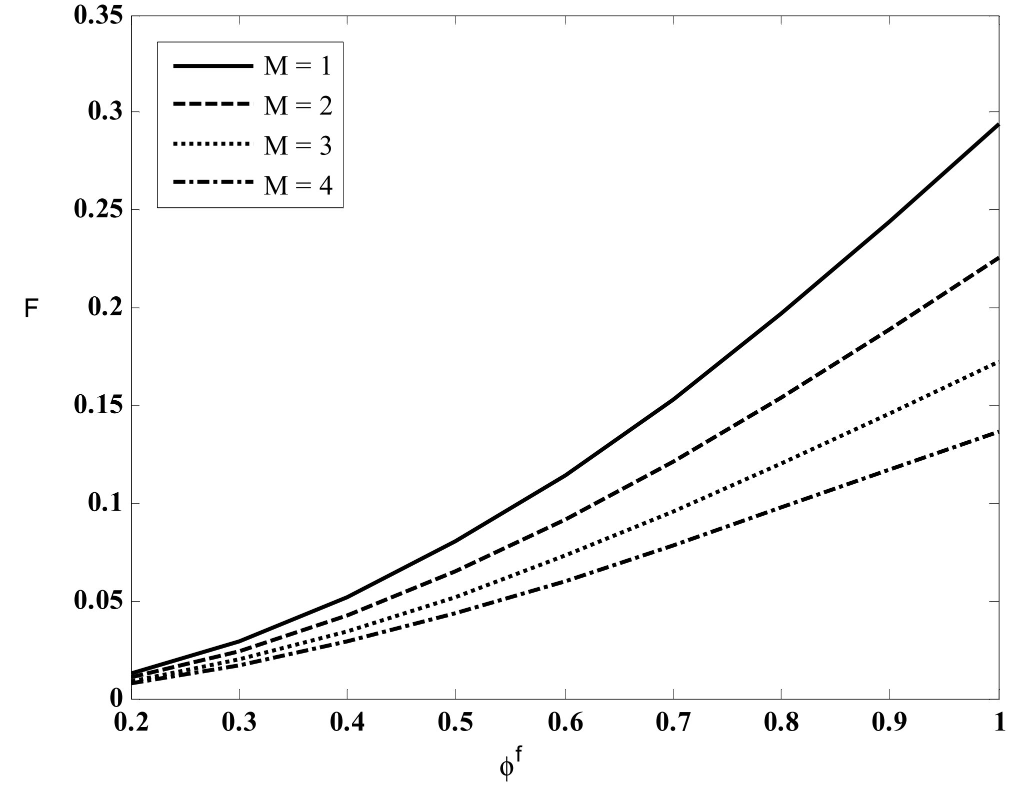

Figure 16 Variation of F with φ^f for different values of M .

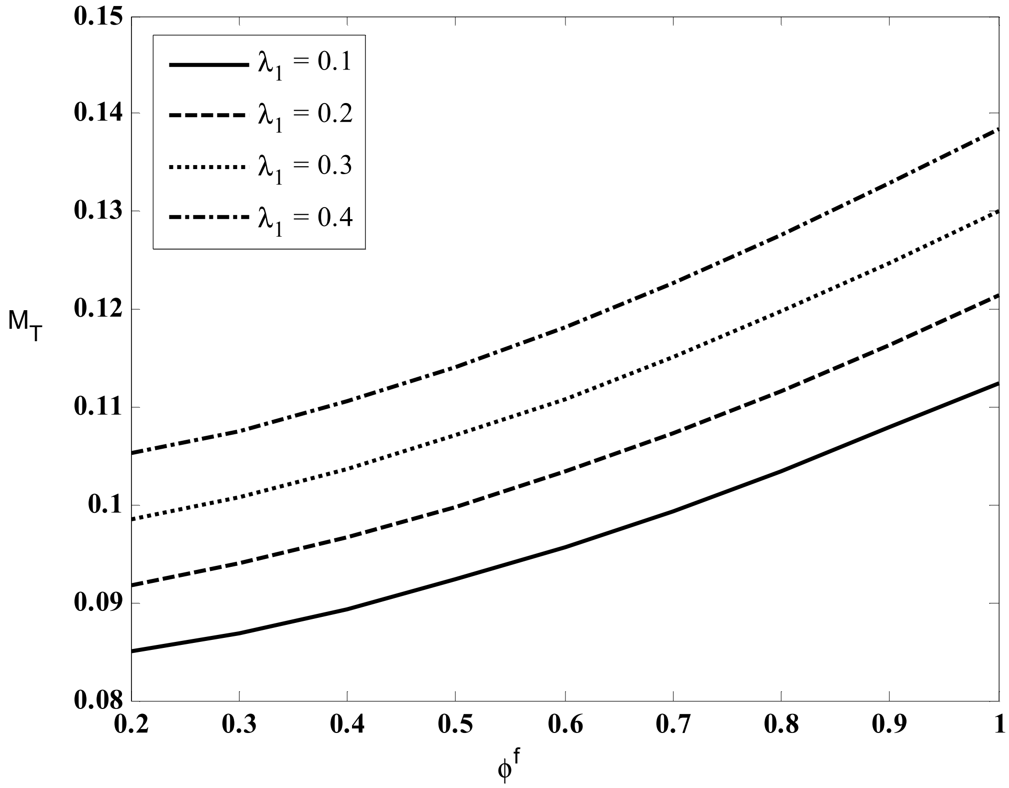

Figure 17 Variation total mass flow rate M_T with φ^f for different values of λ_1 .

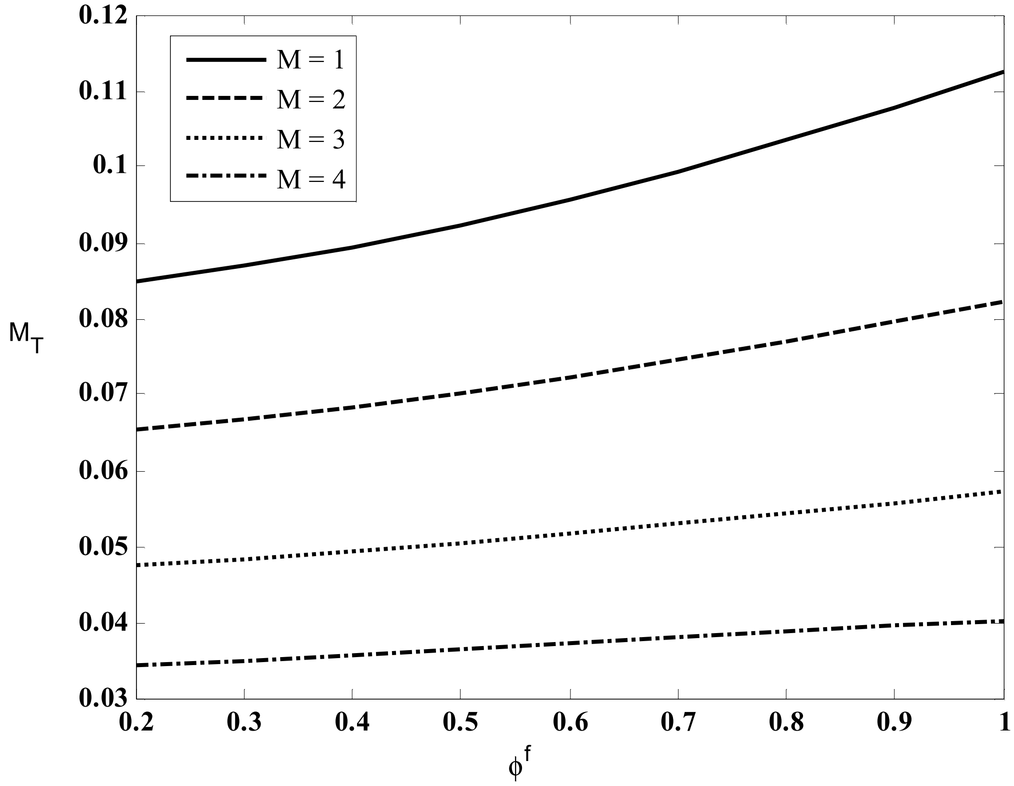

Figure 18 Variation total mass flow rate M_T with φ^f for different values of M .

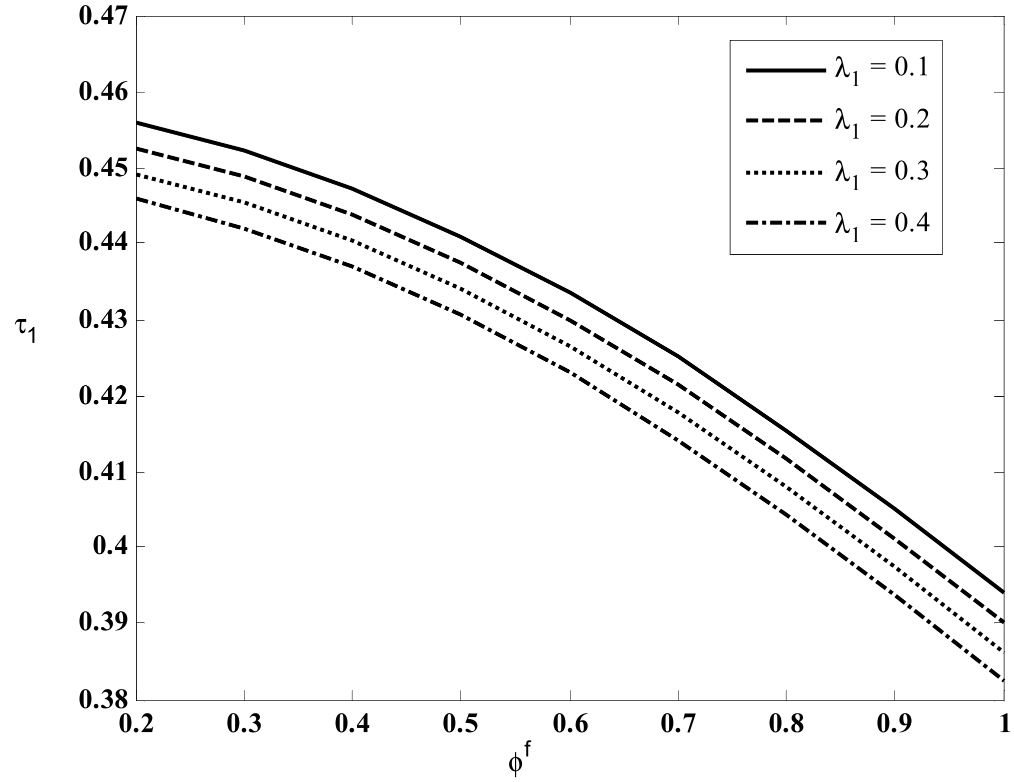

Figure 19 Variation of τ_1 with φ^f for different values of λ_1 .

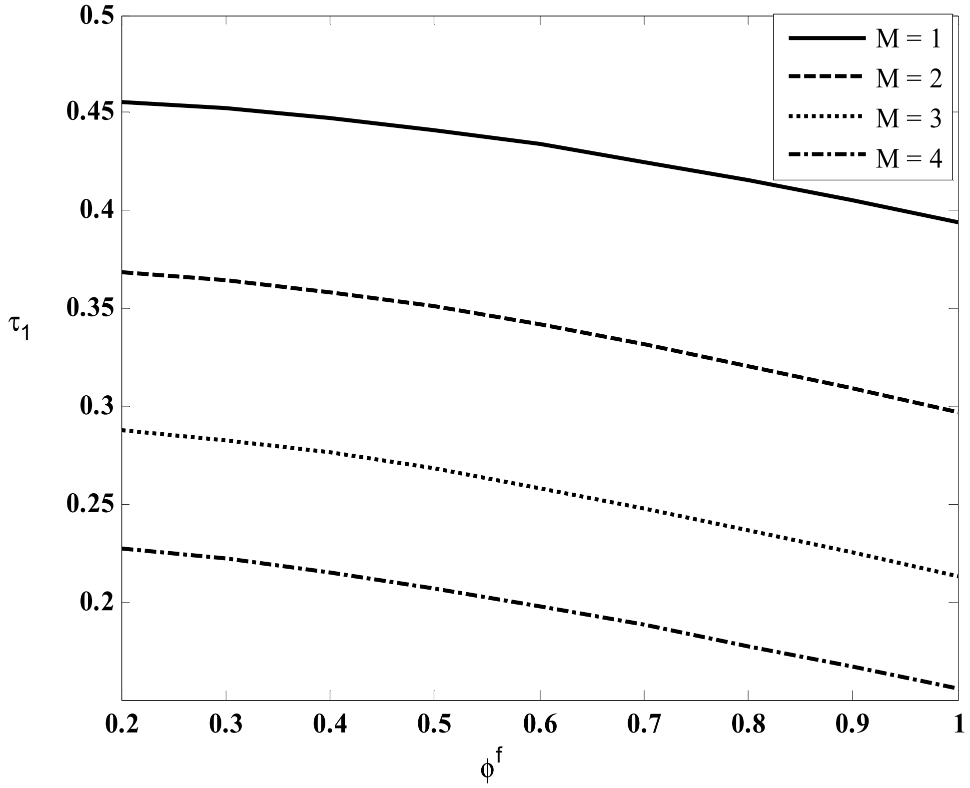

Figure 20 Variation of τ_1 with φ^f for different values of M .